HEP-TH/9609067, KYUSHU-HET-33

# Nonperturbative renormalization group in a light-front three-dimensional real scalar model

Takanori Sugihara *

*Department of Physics, Kyushu University, Fukuoka 812-81, Japan*

Masanobu Yahiro †

*University of Fisheries, Shimonoseki 759-65, Japan*

(February 1, 2008)



## Abstract

The three-dimensional real scalar model, in which the $Z_2$ symmetry spontaneously breaks, is renormalized in a nonperturbative manner based on the Tamm-Dancoff truncation of the Fock space. A critical line is calculated by diagonalizing the Hamiltonian regularized with basis functions. The marginal ($\phi^6$) coupling dependence of the critical line is weak. In the broken phase the canonical Hamiltonian is tachyonic, so the field is shifted as $\phi(x) \to \varphi(x) + v$. The shifted value $v$ is determined as a function of running mass and coupling so that the mass of the ground state vanishes.

PACS numger(s):11.10.G, 11.10.H, 11.10.S, 11.30.Q



*e-mail : taka@higgs.phys.kyushu-u.ac.jp

†e-mail : yahiro@fish-u.ac.jp

## I. INTRODUCTION

Although the field theory has been studied for a long time, we have no complete understanding of relativistic bound state problems. We have to solve the quantum chromodynamics (QCD) nonperturbatively to investigate low-energy hadronic physics. The most reasonable nonperturbative method for such a problem is the lattice gauge theory. In the method, it is easy to calculate the lightest particle state, but not to evaluate the excited and scattering states. Although there exist many nonperturbative prescriptions in the Hamiltonian formalism, the formalism has been abandoned so far since Lorentz invariance and the renormalizability are not obvious.

The light-front (LF) Tamm-Dancoff field theory [1] is known as a method based on the Hamiltonian formalism. The Hamiltonian is constructed by quantizing fields on the light-cone and truncating the Fock space. The truncation is called the Tamm-Dancoff approximation [2]. The completeness of the Fock space is approximated as $\sum_{n=1}^{N_{\rm TD}} |n\rangle\langle n| \sim 1$, where $N_{\rm TD} \to \infty$ corresponds to the full theory. It is possible to calculate mass spectra nonperturbatively by diagonalizing the Hamiltonian in the space. The resulting mass spectrum seems to be accurate for low-lying states, since the pair creation and annihilation are suppressed in the LF field theory [3], especially the pair creation of particles from the LF vacuum is kinematically prohibited. The prohibition warrants the truncation to be reliable. This is an advantage of this method, but, at the same time, it causes a problem. No pair creation means that the vacuum is trivial $H|0\rangle = 0$, i.e., the vacuum is always symmetric in the LF field theory. This causes serious problems, because various phenomena are explained as results of spontaneous symmetry breaking (SSB) in the relativistic field theory. How can the LF field theory describe SSB? It has been said that the zero-mode operator leads the LF field theory to SSB [4,5]. We have a constraint equation for the zero-mode, if the system is quantized in a box with a periodic boundary condition. New interactions induced by the zero-mode affect the renormalization [6], independently of whether the symmetry breaks spontaneously or not. A relation between the zero-mode scenario and the conven-

tional understanding based on the effective potential in the equal-time field theory is not clarified yet. There are several works [7] for the two-dimensional real scalar model, in which the zero-mode constraint equation is solved under reasonable approximations to describe SSB of the $Z_2$ symmetry. At least for the two-dimensional case, the light-front formulation seems to be consistent with the equal-time one, if the zero-mode contributions are treated properly. This approach to SSB has never been applied to higher dimensional models having ultraviolet divergences.

According to our previous work [8] based on perturbation, the canonical Hamiltonian yields a tachyonic spectrum for the broken phase owing to renormalization effects. We have to expand the field around the correct vacuum expectation value (VEV) to restore positivity of the spectrum. There exists an RG invariant relation among VEV and running parameters, and the VEV is determined from the relation as a function of the original parameters. The broken phase is an RG invariant surface containing the critical line in the parameter space. The symmetry breaking interactions were originally introduced by Perry and Wilson in the coupling coherence study [9,10], but the instability of the canonical Hamiltonian was not mentioned.

In this paper, we treat the real scalar model in three dimensions and propose a nonperturbative RG prescription based on the Tamm-Dancoff truncation. The theory is regularized by expanding wavefunctions in terms of basis functions in a truncated momentum space. The mass spectrum is then obtained by diagonalizing the Hamiltonian within a space spanned by the basis functions. In actual calculations we take the Fock space up to three-body states. It is discussed through wave functions whether the truncated space is large enough. The marginal coupling dependence of the critical line is also analyzed. A proper Hamiltonian for the broken phase is constructed by shifting the field as $\phi(x) \to \varphi(x) + v$. A relation of $v$ to the original parameters are nonperturbatively determined by searching the critical surface which gives a vanishing mass for the ground state.

The paper is organized as follows. In section II, a qualitative aspect of mass spectra in the three-dimensional real scalar model is shown with perturbative Bloch-Horowitz RG

analysis. In section III, a regularization based on basis functions is introduced. In section IV, numerical RG is carried out by using the nonperturbative regularization mentioned above. The section V is devoted to discussions.

Notational conventions are summarized as $x^{\pm} = (x^0 \pm x^2)/\sqrt{2}$, time $x^+$, space $(x^-, x_\perp)$, momentum $\mathbf{k} \equiv (k^+, k_\perp)$, metric $g^{+-} = g_{+-} = -g^{11} = -g_{11} = 1$ and others $= 0$, and LF energy $k^- = \epsilon(\mathbf{k}) \equiv (k_\perp^2 + r)/2k^+$, where $r$ is a mass parameter.

## II. SHIFTED FIELD AND POSITIVE DEFINITE HAMILTONIAN

Let us consider a Hamiltonian regularized with some cut-off $\Lambda_n$ in order for a divergent theory to be well-defined. The Einstein-Schrödinger (ES) equation for the Hamiltonian is

$$H(r_n, \lambda_n, \ldots; \Lambda_n)|\Psi\rangle = E|\Psi\rangle, \tag{2.1}$$

where $r_n, \lambda_n, \ldots$ are running parameters belonging to the model. We need a certain transformed Hamiltonian which has a lowered cutoff $\Lambda_{n+1}(\Lambda_{n+1} < \Lambda_n)$ and gives the same eigenvalue $E$,

$$H'(r_{n+1}, \lambda_{n+1}, \ldots; \Lambda_{n+1})|\Psi'\rangle = E|\Psi'\rangle. \tag{2.2}$$

We are now looking for a prescription to get transformed parameters $r_{n+1}, \lambda_{n+1}$ which include radiative corrections. To do that, we use the following projection operators [11],

$$\mathcal{P} = \theta(\Lambda_{n+1}^2 - M_{\rm int}^2), \quad \mathcal{Q} = \theta(M_{\rm int}^2 - \Lambda_{n+1}^2), \tag{2.3}$$

where $M_{\rm int}$ is a total invariant mass ($M_{\rm int}^2 = P^2$) of an intermediate Fock state. The transformed Hamiltonian, which gives a correct spectrum in the $\mathcal{P}$ space, can be written formally as,

$$H' = \mathcal{P}H\mathcal{P} + \mathcal{P}V\mathcal{Q}\frac{1}{E - H}\mathcal{Q}V\mathcal{P}, \quad |\Psi'\rangle = \mathcal{P}|\Psi\rangle. \tag{2.4}$$

This Hamiltonian $H'$ is called the Bloch-Horowitz effective Hamiltonian and used in many-body problem for the purpose of reduction of the degrees of freedom which are too much

to treat it directly [12]. We expect that this Hamiltonian effectively describes physics near the ground state. Expanding the term $1/(E-H)$ with respect to the coupling constant, integrating over the higher invariant mass space $\mathcal{Q}$ and rescaling the lowered cutoff $\Lambda_{n+1}$ to the original one $\Lambda_n$, we can write down RG equations for all parameters [13]. The effective Hamiltonian, however, contains a problem. The resultant RG equations seems to depend on the energy $E$ at a sight. In our previous work [8], we have shown perturbatively for the four-dimensional $\phi^4$ model that the energy dependence of RG equation is negligible at one-loop order if the cutoff is sufficiently large. It's not clear whether it is true or not beyond perturbation. In this paper, we use the effective Hamiltonian (2.4) only in order to explain qualitative effects of RG on mass spectra perturbatively.

Next, we derive a perturbative RG equation for mass parameter in the three-dimensional real scalar model. We assume that the Lagrangian density is

$$\mathcal{L} = \frac{1}{2}\partial_\mu\phi\partial^\mu\phi - \frac{r}{2}\phi^2 - \frac{\lambda}{4!}\phi^4 - \frac{w}{6!}\phi^6. \tag{2.5}$$

The field is quantized as

$$[\phi(x), \phi(y)]_{x^+=y^+} = -\frac{i}{4}\epsilon(x^- - y^-)\delta(x_\perp - y_\perp), \tag{2.6}$$

if the zero-mode is neglected. The factor $1/4$ on the right-hand side of Eq. (2.6) is from the Poisson bracket

$$\{\Phi(x), \Phi(y)\}_{x^+=y^+} = (-\partial_-^x + \partial_-^y)\delta(x^- - y^-)\delta(x_\perp - y_\perp), \tag{2.7}$$

where $\Phi(x) = \pi(x) - \partial_-\phi(x)$ is a primary constraint and $\pi$ is conjugate to $\phi$. The canonical Hamiltonian is given by,

$$H_{\rm S} = \int d^2x \left(\frac{1}{2}(\partial_\perp\phi)^2 + \frac{r}{2}\phi^2 + \frac{\lambda}{4!}\phi^4 + \frac{w}{6!}\phi^6\right). \tag{2.8}$$

The normal ordering is taken here. This is equivalent to renormalization of tad-pole diagrams by redefining parameters. We have to include various kinds of relevant and marginal interactions to renormalize all new interactions produced by RG transformations. Our Hamiltonian

is assumed to have three interactions included in Eq. (2.8). The mass renormalization is most important, because $r$ is most relevant to mass spectra. It is the kinetic term which mainly contributes to mass spectra especially in the perturbative region. The RG equation for mass $r$ is given with perturbation as

$$r_{n+1} = L^2 \left( r_n + \frac{B}{192\pi^2} \lambda_n^2 \right) + O(\lambda_n^3), \tag{2.9}$$

where

$$B \equiv \int \left[ \prod_{i=1}^{3} \frac{d^2 k_i}{k_i^+} \right] \delta^2(\mathbf{P} - \sum_{i=1}^{3} \mathbf{k}_i) \left( E - \sum_{i=1}^{3} \epsilon(\mathbf{k}_i) \right)^{-1}, \quad L \equiv \frac{\Lambda_n}{\Lambda_{n+1}}. \tag{2.10}$$

It is understood implicitly that the loop integral is made in the $\mathcal{Q}$ space. The factor $L$ is produced by rescaling the new cutoff $\Lambda_{n+1}$ to the original cutoff $\Lambda_n$. By changing variables to Jacobi coordinates,

$$\mathbf{k}_i = (x_i K^+, x_i K_\perp + s_i), \quad \textstyle\sum_{i=1}^{3} x_i = 1, \quad \sum_{i=1}^{3} s_i = 0,$$
$$0 < x_i < 1, \quad -\infty < s_i < \infty,$$

where all intermediate states have a common total momentum $\mathbf{K}$, the integral $B$ becomes

$$B = 2 \int \frac{dx_1 dx_2 ds_1 ds_2}{x_1 x_2 (1 - x_1 - x_2)} \frac{1}{M^2 - M_{\rm int}^2(x_1, x_2, s_1, s_2)}, \tag{2.11}$$

where $M$ is an external mass (an eigenvalue of Hamiltonian) and $M_{\rm int}$ a mass in the intermediate Fock state,

$$M_{\rm int}^2(x_1, x_2, s_1, s_2) \equiv \frac{s_1^2 + r_n}{x_1} + \frac{s_2^2 + r_n}{x_2} + \frac{(s_1 + s_2)^2 + r_n}{1 - x_1 - x_2}. \tag{2.12}$$

It is assumed that the external mass $M$ is small compared to the cutoff scale. The intermediate mass $M_{\rm int}$ is large because it sits in the higher mass space $\mathcal{Q}$. Then, $M^2$ is much smaller than $M_{\rm int}^2$. This assumption is reasonable for the purpose to calculate a critical line and draw a phase diagram. We can observe from $B$ being negative that $\lim_{n\to\infty} r_n = \infty$ if the initial value $r_0$ is sufficiently large and $\lim_{n\to\infty} r_n = -\infty$ if the initial value $r_0$ is small. That is, there exist a critical line $r = r_{\rm c}(\lambda)$ in the first quadrant of the two dimensional parameter

space $(r, \lambda)$, and $r > r_c(\lambda)$ and $r < r_c(\lambda)$ correspond to symmetric and asymmetric phases respectively. In the asymmetric phase, the canonical Hamiltonian (2.8) is tachyonic, i.e., square of eigenmass is not bounded from below although Hamiltonian should be positive definite. Positivity of the spectrum is restored by expanding the field $\phi$ around the correct VEV $v$. Substituting $\phi(x) = \varphi(x) + v$ into Eq. (2.8), we have

$$H_{\rm A} = H_0 + H_1, \tag{2.13}$$

$$H_0 = \int d^2x \frac{1}{2}\left((\partial_\perp \varphi)^2 + g_2\varphi^2\right), \tag{2.14}$$

$$H_1 = \int d^2x \sum_{i=3}^{6} \frac{g_n}{n!}\varphi^n, \tag{2.15}$$

where the new mass parameter is

$$g_2 \equiv r + \frac{\lambda v^2}{2} + \frac{wv^4}{24}, \tag{2.16}$$

and the new coupling constants are

$$g_3 \equiv (\lambda + \frac{wv^2}{6})v, \quad g_4 \equiv \lambda + \frac{wv^2}{2}, \quad g_5 \equiv wv, \quad g_6 \equiv w. \tag{2.17}$$

The $v$ is just a free parameter at this stage. We have three parameters in the symmetric Hamiltonian $H_{\rm S}$ and four in the asymmetric one $H_{\rm A}$. The RG parameter space for $H_{\rm A}$ is larger than that for $H_{\rm S}$. The $v$ should be a function of the original three parameters belonging to $H_{\rm S}$, that is, there should exist an RG invariant relation among the four parameters. Actually, following our previous work [8] for the real scalar model in four dimensions, we can find out the same RG invariant relation $6r + \lambda v^2 = 0$ also for the three-dimensional case, with perturbative renormalization at one-loop order, if the $\phi^6$ interaction is neglected. The neglect of the marginal operator will be justified by numerical analyses shown later. The RG invariant relation forms a surface in the parameter space of $H_{\rm A}$. All asymmetric Hamiltonians on the surface describe physics for the broken phase. All running parameters on the surface go to zero in the limit $\Lambda \to 0$ which corresponds to infinite iterations of RG transformation, satisfying the RG invariant relation $6r + \lambda v^2 = 0$. The Hamiltonian $H_{\rm A}$ thus gives massless spectrum in the limit. All Hamiltonians on the surface converge to the

same massless Hamiltonian in the limit, indicating that $H_{\rm A}$ gives massless spectrum at any point on the surface. It is known for the real scalar models in three and four dimensions that the effective potential is convex and has flat bottom in the broken phase [14]. We may choose any point in the flat region as a stable vacuum. It is likely that this fact supports the existence of a massless particle in the broken phase. We will continue our analysis with the fact in mind, that is, we find out the broken phase nonperturbatively by searching massless eigenvalues.

## III. BASIS FUNCTION REGULARIZATION

The first principle of RG is to find a flow which gives the same physics. It is not easy to calculate the effective interaction part of the Bloch-Horowitz Hamiltonian directly for our practical purpose of nonperturbative renormalization and we have to avoid energy dependences of renormalization, then we consider another approach. In our framework, we can draw RG flows by calculating spectra. We regularize the LF Hamiltonian with the basis function regularization and try to calculate the critical line and the critical surface.

In general, we can express an arbitrary state in the Fock space such as

$$|\Psi(\mathbf{P})\rangle = \sum_{n=1}^{N_{\rm TD}} \frac{1}{\sqrt{n!}} \int \left[\prod_{i=0}^{n} d^2k_i\right] \delta^2(\mathbf{P} - \sum_{i=1}^{n} \mathbf{k}_i)\psi_n(\mathbf{k}_1, \mathbf{k}_2, \ldots, \mathbf{k}_n) \prod_{i=0}^{n} a^\dagger(\mathbf{k}_i)|0\rangle, \tag{3.1}$$

where $\mathbf{P}$ is the total momentum of the state and the wavefunction $\psi_n$ is symmetric under exchanges of arbitrary two momenta. The limit $N_{\rm TD} \to \infty$ corresponds to the full theory and the state is normalized as

$$\langle\Psi(\mathbf{P})|\Psi(\mathbf{Q})\rangle = \delta^2(\mathbf{P} - \mathbf{Q}). \tag{3.2}$$

We will set a certain small number to $N_{\rm TD}$, which is called the Tamm-Dancoff approximation. In this paper, the Fock space is truncated up to three body states ($N_{\rm TD} = 3$). According to the variational principle, the mass spectrum in the truncated Fock space is given by solving (diagonalizing) the ES equation

$$P^2|\Psi(\mathbf{P})\rangle = M^2|\Psi(\mathbf{P})\rangle. \tag{3.3}$$

We introduce a cutoff $\Lambda$ and show the present regularization scheme later. All quantities belonging to the model are measured in units of the $\Lambda$ and attached tilde. In units of the cutoff, eigenmass and running parameters are

$$\tilde{M} \equiv M/\Lambda, \quad \tilde{v} \equiv v/\Lambda^{1/2}, \quad \tilde{r} \equiv r/\Lambda^2, \quad \tilde{\lambda} \equiv \lambda/\Lambda, \quad \tilde{w} \equiv w, \tag{3.4}$$

then

$$\tilde{g}_n = g_n/\Lambda^{(6-n)/2}. \tag{3.5}$$

The $\phi^6$ interaction is marginal as shown in Eq. (3.5). We will check the marginal coupling dependence of the critical line in the next section. The momentum is also redefined as

$$\mathbf{x}_i = (x_i, X_i) \equiv (k_i^+/P^+, k_{i\perp}/\Lambda), \tag{3.6}$$

where $0 < x_i < 1$ since $k_i^+ > 0$. In this rescaled notation, the normalization condition Eq. (3.2) of the wavefunction becomes

$$\sum_{n=1}^{N_{\rm TD}} \int \left[\prod_{i=1}^{n} d\mathbf{x}_i\right] \delta^2(\tilde{\mathbf{P}} - \sum_{i=1}^{n} \mathbf{x}_i)|\tilde{\psi}_n(\mathbf{x}_1, \mathbf{x}_2, \ldots, \mathbf{x}_n)|^2 = 1, \tag{3.7}$$

where

$$\tilde{\mathbf{P}} \equiv (1, \tilde{P}_\perp) = (1, P_\perp/\Lambda), \tag{3.8}$$

and the rescaled wavefunctions are

$$\tilde{\psi}_n(\mathbf{x}_1, \mathbf{x}_2, \ldots, \mathbf{x}_n) \equiv \left(P^+\Lambda\right)^{\frac{n-1}{2}} \psi_n(\mathbf{k}_1, \mathbf{k}_2, \ldots, \mathbf{k}_n). \tag{3.9}$$

The ES equation in the rescaled notation is given in appendix B. It can be seen that the ES equation does not depend on the longitudinal momentum $P^+$ and the cutoff $\Lambda$.

Regularization of transverse momenta and discretization of Fock space are closely related to each other. The regularization of the Hamiltonian is realized as a boundary condition of the wavefunctions. That is, we solve this eigenvalue problem, keeping the constraint that

the transverse component of $\tilde{\psi}_3$ is zero at edges ($X_i = -1, 1$). The ES equation is regularized with the naive transverse cutoff,

$$-\Lambda < k_{i\perp} < \Lambda \leftrightarrow -1 < X_i < 1, \tag{3.10}$$

since the ultraviolet divergence is caused by the transverse loop integral. The Fock space is discretized by expanding the wavefunction in terms of basis functions in the momentum space ($-1 < X_i < 1, \quad 0 < x_i < 1$),

$$\tilde{\psi}_n(\mathbf{x}_1, \mathbf{x}_2, \ldots, \mathbf{x}_n) = \sum_{\mathbf{k}=0}^{N_{\rm L}(n)} \sum_{\mathbf{l}=0}^{N_{\rm T}(n)} a_{\mathbf{kl}}^{(n)} \mathcal{S}_{1,2,\ldots,n} \left[ \prod_{i=1}^{n} f_{k_i}(x_i) F_{l_i}(X_i) \right], \tag{3.11}$$

where

$$\sum_{i=1}^{n} x_i = 1, \quad \sum_{i=1}^{n} X_i = \tilde{P}_\perp, \tag{3.12}$$

and $\mathcal{S}_{1,2,\ldots,n}$ is a symmetrizer. The $N_{\rm L}(n)$ and $N_{\rm T}(n)$ are taken sufficiently large so that the eigenvalue of the ground state can converge. Longitudinal basis functions are

$$f_k(x) = x^{\beta(n)+k}, \quad 0 < x < 1, \tag{3.13}$$

for $0 < \beta(n) < 1$ and transverse basis functions are

$$F_l(X) = (1 - X^2)X^l, \quad -1 < X < 1. \tag{3.14}$$

The variational parameter $\beta(n)$ is tuned so that the ground state takes minimum eigenvalue. The behavior of the three-body wavefunction near the edges ($x = 0, 1$) is important because of the kinetic term proper to LF [15,3]. The coefficients $a_{\mathbf{kl}}^{(n)}$ are determined by diagonalizing the Hamiltonian in the momentum space spanned by the basis functions. Mathematically, Eq. (3.3) has exact eigenvalues only in the case that the functional space is expanded in terms of the complete set of basis functions. We can get only upper bounds of eigenvalues, since the wavefunction is expanded in terms of incomplete basis functions in this calculation. However, we expect that the spectrum is described accurately for low-lying states, since shapes of the wavefunctions are simple; for example, the calculated wavefunction of the ground state has no node.

In this paper, a phase diagram which includes rescaling effects is evaluated, in accordance with Wilson's RG prescription [13]. It is not needed to vary the cutoff because the transformed cutoff is rescaled to the original one in this RG. Parameter sets which give the same eigenvalue are calculated for a fixed cutoff.

The wavefunction renormalization is neglected in this calculation, i.e., $Z_\varphi = 1$. The phase diagram is dominated by the Gaussian fixed point, since the field is rescaled according to the canonical dimension. In order to find a non-trivial fixed point, we have to consider the wavefunction renormalization. These two phase diagrams, which have trivial and non-trivial fixed points, describe different theories. Our result makes sense as the theory dominated by the Gaussian fixed point.

In this calculation, the total transverse momentum of the eigenstate is set to zero, $\tilde{P}_\perp = 0$, and $N_{\mathrm{L,T}}(n) = 3$ in Eq. (3.11), which is sufficiently large so as to give a convergent spectrum.

## IV. NUMERICAL RESULTS

Mass spectrum is plotted in Fig. 1 for the case $\tilde{\lambda} = 10$ and $\tilde{w} = 0$ without introducing $\tilde{v}$. No multi-bosonic bound state is found in this calculation. We can observe a massless point $\tilde{r}_{\mathrm{c}}(\tilde{\lambda} = 10)$. The point is called the critical point. We can draw the critical line by connecting the critical points which are calculated for various $\tilde{\lambda}$. The critical line is plotted in Fig. 2 for five values of marginal coupling constants, $\tilde{w} = 0, 1, 10, 10^2, 10^3$. Values of two parameters $\tilde{r}$ and $\tilde{\lambda}$ which form the critical lines are tabulated in table I for each $\tilde{w}$. The dependence of the line on $\tilde{w}$ is weak. This is consistent with our intuition based on perturbative analysis, i.e., the dependence of the line on higher power operators in $\varphi$ may be week. After this, we will switch off the marginal coupling ($\tilde{w} = 0$), and draw the phase diagram of three running parameters, $\tilde{v}$, $\tilde{r}$ and $\tilde{\lambda}$ near the $\tilde{v} = 0$ plane.

The lowest eigenmass is zero on the line, corresponding to an infinite correlation length in the statistical theoretical language. The spectrum of the canonical Hamiltonian is not bounded from below in the left region of the critical line. We then conclude that excited

states are lighter than the ground state in the region if we solve the canonical Hamiltonian as it is. This is a result of the mass renormalization effect explained in the section II. The true Hamiltonian should be positive definite even in the left region of the critical line. It is natural to introduce the VEV in the broken phase in order to construct a positive definite Hamiltonian. The symmetry has to be spontaneously broken for the spectrum to keep positive. Figure 3(a) shows a relation $\tilde{\lambda}\tilde{v}^2+6\tilde{r}=0$ among three parameters $\tilde{v}$, $\tilde{r}$ and $\tilde{\lambda}$, which is given by perturbative RG calculations at one-loop order; the detail of the calculations is shown in [8] for the case of the four-dimensional scalar model. We can see a critical line on the positive $\tilde{\lambda}$ axis, which is trivial because no renormalization effect is included. In Fig. 3(b), a critical surface is drawn. The surface is calculated by searching points which give massless spectrum in the three-dimensional parameter space $(\tilde{v}, \tilde{r}, \tilde{\lambda})$. Positivity of the Hamiltonian is restored by introducing $\tilde{v}$. Compared to the surface (a) in Fig. 3, the surface (b) slants to the positive $\tilde{r}$ direction if $\tilde{v}$ is small and to the negative direction if $\tilde{v}$ is large, as a result of renormalization effects.

Components of the ground state wavefunction on the critical line shown in Fig. 2 are plotted in Fig. 4 in order to confirm whether the TD approximation works well or not. One- and three-body wavefunction probabilities are plotted as a function of $\tilde{\lambda}$ on the critical line. The three-body component is very small even for comparatively strong coupling $\tilde{\lambda}$. This means that the spectrum does not change near the critical line even if higher Fock space contributions are included in the calculation. This is true also in region far from the critical line, when the VEV is zero. The three-body component of the ground state wavefunction tends to decrease, as mass parameter increases with coupling constant fixed, because taking large mass parameter is effectively the same as taking weak coupling constant.

Next, we investigate TD dependence of the critical surface. Figure 5 shows wavefunction components of the ground state on the intersection between the critical surface and the $\tilde{\lambda}=50$ plane. The coupling constant is set to the largest value in this calculation. One- and two-body components are dominant and three-body component is small also in this case. The two-body component increases rapidly near $\tilde{v}=0.1$, whereas the three-body component

increases slowly and keeps values around a few percent. It is expected near the $\tilde{v} = 0$ plane that the Tamm-Dancoff approximation is good.

## V. SUMMARY AND DISCUSSIONS

We have shown how to renormalize the Hamiltonian nonperturbatively for the three-dimensional real scalar model and calculated the critical line and the critical surface. There exist a region where the canonical Hamiltonian $H_{\rm S}$ is unstable independently of perturbation. The mass spectrum is tachyonic in the left region of the critical line. We have then introduced VEV to restore instability of the Hamiltonian and calculated the critical surface. The asymmetric Hamiltonian $H_{\rm A}$ on the surface describes physics for the broken phase, if the phase has a massless mode. This is precisely true for SSB of any continuous symmetry, and the present approach for finding the broken phase is applicable for the case. Similarly to the present bosonic case, there seems to exist a region where Hamiltonian is unstable if we renormalize a mass term $m\bar{\psi}\psi$ in fermionic theories. It is reasonable to understand that the instability is restored by introducing VEV of a bosonic field.

The marginal coupling dependence of the critical line is weak. This result links to the fact that the Tamm-Dancoff approximation up to three-body state works well. The ES equation for $\tilde{\psi}_1$ has no marginal interaction, but the ES equation for $\tilde{\psi}_3$ has that. The ground state has marginal coupling dependence only through the three-body wavefunction $\tilde{\psi}_3$ which is extremely small as a result of nonperturbative calculation. This is the reason why the marginal coupling dependence of the ground state is weak.

This RG program seems to be independent of energy eigenvalues. In order to check this, we need plural number of bound states. For example, we can use spin singlet and degenerate triplet states in a fermionic theory such as Yukawa model. It is possible to draw RG flows by using a spectrum of one-body fermionic state in a similar way which has been done in this paper. We can say that the RG is energy independent if the spectra of the spin singlet and triplet states are renormalized with the same RG flow.

## VI. ACKNOWLEDGMENTS

We would like to thank K. Harada and S. Tominaga for helpful discussions.

## APPENDIX A: OSCILLATOR EXPANSION OF THE FIELD

The field $\varphi$ is expanded at $x^+ = 0$ with oscillators as

$$\varphi(x)_{x^+=0} = \int_0^\infty dk^+ \int_{-\infty}^\infty \frac{dk_\perp}{\sqrt{2k^+(2\pi)^2}} \left[ a(\mathbf{k}) e^{-ik^+x^- + ik_\perp x_\perp} + a^\dagger(\mathbf{k}) e^{ik^+x^- - ik_\perp x_\perp} \right], \tag{A1}$$

where

$$\left[ a(\mathbf{k}), a^\dagger(\mathbf{k}') \right] = \delta^2(\mathbf{k} - \mathbf{k}'). \tag{A2}$$

## APPENDIX B: EINSTEIN SCHRÖDINGER EQUATION

The ES equation (3.3) becomes

$$\begin{aligned}
&\tilde{M}^2 \tilde{\psi}_n(\mathbf{x}_1, \mathbf{x}_2, \ldots, \mathbf{x}_n) \qquad (B1)\\
&= \left[ \sum_{i=1}^n \tilde{\epsilon}(\mathbf{x}_i) - \tilde{\mathbf{P}}_\perp^2 \right] \tilde{\psi}_n(\mathbf{x}_1, \mathbf{x}_2, \ldots, \mathbf{x}_n) \\
&+ \frac{\tilde{g}_4}{4!} \frac{6}{(2\pi)^2} \int_{\mathbf{y}} \sum_{i<j}^n \frac{\delta^2(\mathbf{x}_i + \mathbf{x}_j - \sum_{i=1}^2 \mathbf{y}_i)}{\sqrt{x_i x_j}} \\
&\qquad \times \tilde{\psi}_n(\mathbf{y}_1, \mathbf{y}_2, \mathbf{x}_1, \ldots, \check{\mathbf{x}}_i, \ldots, \check{\mathbf{x}}_j, \ldots, \mathbf{x}_n) \\
&+ \frac{\tilde{g}_6}{6!} \frac{30}{(2\pi)^4} \int_{\mathbf{y}} \sum_{i<j<k}^n \frac{\delta^2(\mathbf{x}_i + \mathbf{x}_j + \mathbf{x}_k - \sum_{i=1}^3 \mathbf{y}_i)}{\sqrt{x_i x_j x_k}} \\
&\qquad \times \tilde{\psi}_n(\mathbf{y}_1, \mathbf{y}_2, \mathbf{y}_3, \mathbf{x}_1, \ldots, \check{\mathbf{x}}_i, \ldots, \check{\mathbf{x}}_j, \ldots, \check{\mathbf{x}}_k, \ldots, \mathbf{x}_n) \\
&+ \frac{\tilde{g}_3}{3!} \frac{3}{\sqrt{2}(2\pi)} \sqrt{\frac{(n+1)!}{n!}} \int_{\mathbf{y}} \sum_{i=1}^n \frac{\delta^2(\mathbf{x}_i - \sum_{i=1}^2 \mathbf{y}_i)}{\sqrt{x_i}} \\
&\qquad \times \tilde{\psi}_{n+1}(\mathbf{y}_1, \mathbf{y}_2, \mathbf{x}_1, \ldots, \check{\mathbf{x}}_i, \ldots, \mathbf{x}_n) \\
&+ \frac{\tilde{g}_5}{5!} \frac{10}{\sqrt{2}(2\pi)^3} \sqrt{\frac{(n+1)!}{n!}} \int_{\mathbf{y}} \sum_{i<j}^n \frac{\delta^2(\mathbf{x}_i + \mathbf{x}_j - \sum_{i=1}^3 \mathbf{y}_i)}{\sqrt{x_i x_j}} \\
&\qquad \times \tilde{\psi}_{n+1}(\mathbf{y}_1, \mathbf{y}_2, \mathbf{y}_3, \mathbf{x}_1, \ldots, \check{\mathbf{x}}_i, \ldots, \check{\mathbf{x}}_j, \ldots, \mathbf{x}_n)
\end{aligned}$$

$$
\begin{aligned}
&+\frac{\tilde{g}_3}{3!}\frac{6}{\sqrt{2}(2\pi)}\sqrt{\frac{(n-1)!}{n!}}\int_{\mathbf{y}}\sum_{i<j}^{n}\frac{\delta^2(\mathbf{x}_i+\mathbf{x}_j-\mathbf{y})}{\sqrt{x_i x_j}}\\
&\qquad\times\tilde{\psi}_{n-1}(\mathbf{y},\mathbf{x}_1,\ldots,\check{\mathbf{x}}_i,\ldots,\check{\mathbf{x}}_j,\ldots,\mathbf{x}_n)\\
&+\frac{\tilde{g}_5}{5!}\frac{30}{\sqrt{2}(2\pi)^3}\sqrt{\frac{(n-1)!}{n!}}\int_{\mathbf{y}}\sum_{i<j<k}^{n}\frac{\delta^2(\mathbf{x}_i+\mathbf{x}_j+\mathbf{x}_k-\mathbf{y})}{\sqrt{x_i x_j x_j}}\\
&\qquad\times\tilde{\psi}_{n-1}(\mathbf{y}_1,\mathbf{y}_2,\mathbf{x}_1,\ldots,\check{\mathbf{x}}_i,\ldots,\check{\mathbf{x}}_j,\ldots,\check{\mathbf{x}}_k,\ldots,\mathbf{x}_n)\\
&+\frac{\tilde{g}_4}{4!}\frac{2}{(2\pi)^2}\sqrt{\frac{(n+2)!}{n!}}\int_{\mathbf{y}}\sum_{i=1}^{n}\frac{\delta^2(\mathbf{x}_i-\sum_{i=1}^{3}\mathbf{y}_i)}{\sqrt{x_i}}\\
&\qquad\times\tilde{\psi}_{n+2}(\mathbf{y}_1,\mathbf{y}_2,\mathbf{y}_3,\mathbf{x}_1,\ldots,\check{\mathbf{x}}_i,\ldots,\mathbf{x}_n)\\
&+\frac{\tilde{g}_6}{6!}\frac{15}{2(2\pi)^4}\sqrt{\frac{(n+2)!}{n!}}\int_{\mathbf{y}}\sum_{i<j}^{n}\frac{\delta^2(\mathbf{x}_i+\mathbf{x}_j-\sum_{i=1}^{4}\mathbf{y}_i)}{\sqrt{x_i x_j}}\\
&\qquad\times\tilde{\psi}_{n+2}(\mathbf{y}_1,\mathbf{y}_2,\mathbf{y}_3,\mathbf{y}_4,\mathbf{x}_1,\ldots,\check{\mathbf{x}}_i,\ldots,\check{\mathbf{x}}_j,\ldots,\mathbf{x}_n)\\
&+\frac{\tilde{g}_4}{4!}\frac{12}{(2\pi)^2}\sqrt{\frac{(n-2)!}{n!}}\int_{\mathbf{y}}\sum_{i<j<k}^{n}\frac{\delta^2(\mathbf{x}_i+\mathbf{x}_j+\mathbf{x}_k-\mathbf{y})}{\sqrt{x_i x_j x_k}}\\
&\qquad\times\tilde{\psi}_{n-2}(\mathbf{y},\mathbf{x}_1,\ldots,\check{\mathbf{x}}_i,\ldots,\check{\mathbf{x}}_j,\ldots,\check{\mathbf{x}}_k,\ldots,\mathbf{x}_n)\\
&+\frac{\tilde{g}_6}{6!}\frac{90}{(2\pi)^4}\sqrt{\frac{(n-2)!}{n!}}\int_{\mathbf{y}}\sum_{i<j<k<l}^{n}\frac{\delta^2(\mathbf{x}_i+\mathbf{x}_j+\mathbf{x}_k+\mathbf{x}_l-\sum_{i=1}^{2}\mathbf{y}_i)}{\sqrt{x_i x_j x_k x_l}}\\
&\qquad\times\tilde{\psi}_{n-2}(\mathbf{y}_1,\mathbf{y}_2,\mathbf{x}_1,\ldots,\check{\mathbf{x}}_i,\ldots,\check{\mathbf{x}}_j,\ldots,\check{\mathbf{x}}_k,\ldots,\check{\mathbf{x}}_l,\ldots,\mathbf{x}_n)\\
&+\frac{\tilde{g}_5}{5!}\frac{5}{2\sqrt{2}(2\pi)^3}\sqrt{\frac{(n+3)!}{n!}}\int_{\mathbf{y}}\sum_{i=1}^{n}\frac{\delta^2(\mathbf{x}_i-\sum_{i=1}^{4}\mathbf{y}_i)}{\sqrt{x_i}}\\
&\qquad\times\tilde{\psi}_{n+3}(\mathbf{y}_1,\mathbf{y}_2,\mathbf{y}_3,\mathbf{y}_4,\mathbf{x}_1,\ldots,\check{\mathbf{x}}_i,\ldots,\mathbf{x}_n)\\
&+\frac{\tilde{g}_5}{5!}\frac{60}{\sqrt{2}(2\pi)^3}\sqrt{\frac{(n+3)!}{n!}}\int_{\mathbf{y}}\sum_{i<j<k<l}^{n}\frac{\delta^2(\mathbf{x}_i+\mathbf{x}_j+\mathbf{x}_k+\mathbf{x}_l-\mathbf{y})}{\sqrt{x_i x_j x_k x_l}}\\
&\qquad\times\tilde{\psi}_{n-3}(\mathbf{y},\mathbf{x}_1,\ldots,\check{\mathbf{x}}_i,\ldots,\check{\mathbf{x}}_j,\ldots,\check{\mathbf{x}}_k,\ldots,\check{\mathbf{x}}_l,\ldots,\mathbf{x}_n)\\
&+\frac{\tilde{g}_6}{6!}\frac{3}{2(2\pi)^4}\sqrt{\frac{(n+4)!}{n!}}\int_{\mathbf{y}}\sum_{i=1}^{n}\frac{\delta^2(\mathbf{x}_i-\sum_{i=1}^{5}\mathbf{y}_i)}{\sqrt{x_i}}\\
&\qquad\times\tilde{\psi}_{n+4}(\mathbf{y}_1,\mathbf{y}_2,\mathbf{y}_3,\mathbf{y}_4,\mathbf{y}_5,\mathbf{x}_1,\ldots,\check{\mathbf{x}}_i,\ldots,\mathbf{x}_n)\\
&+\frac{\tilde{g}_6}{6!}\frac{180}{(2\pi)^4}\sqrt{\frac{(n-4)!}{n!}}\int_{\mathbf{y}}\sum_{i<j<k<l<m}^{n}\frac{\delta^2(\mathbf{x}_i+\mathbf{x}_j+\mathbf{x}_k+\mathbf{x}_l+\mathbf{x}_m-\mathbf{y})}{\sqrt{x_i x_j x_k x_l x_m}}\\
&\qquad\times\tilde{\psi}_{n-4}(\mathbf{y},\mathbf{x}_1,\ldots,\check{\mathbf{x}}_i,\ldots,\check{\mathbf{x}}_j,\ldots,\check{\mathbf{x}}_k,\ldots,\check{\mathbf{x}}_l,\ldots,\check{\mathbf{x}}_m,\ldots,\mathbf{x}_n),
\end{aligned}
$$

where $\tilde{\epsilon}(\mathbf{x})\equiv(X^2+g_2)/x$ and

$$
\int_{\mathbf{y}}\equiv\int\left[\prod_{i=1}^{n}\frac{d\mathbf{y}_i}{\sqrt{y}_i}\right], \tag{B2}
$$

this shows integrations over $n$-pieces of $\mathbf{y}$, and the $\mathbf{x}$'s with the check symbol are removed from arguments of the wavefunctions. On the right hand side of Eq. (B1), interaction terms in which the number of checked $x$'s is larger than the number of particles $n$ are switched off.

# REFERENCES


[1] R. J. Perry, A. Harindranath, and K. G. Wilson, Phys. Rev. Lett **65**, 2959(1990).

[2] I. Tamm, J. Phys. (USSR)**9**, 449(1945); S. M. Dancoff, Phys. Rev. **78**, 382(1950);

[3] Y. Mo and R. J. Perry, J. Comp. Phys. **108**, 159(1993); K. Harada, T. Sugihara, M. Taniguchi, and M. Yahiro, Phys. Rev. **D49**, 4226(1994); T. Sugihara, M. Matsuzaki, and M. Yahiro, Phys. Rev. **D50**, 5274(1994).

[4] T. Maskawa and K. Yamawaki, Prog. Theo. Phys. **56**, 270(1976).

[5] Y. Kim, S. Tsujimaru, and K. Yamawaki, Phys. Rev. Lett. **74**, 4771(1995).

[6] M. Maeno, Phys.Lett.**B320**,83-90(1994)

[7] C. Bender, S. Pinsky and B. Sande, Phys. Rev. **D48**, 816(1993); S. Pinsky and B. Sande, *ibid*, **49**, 2001(1994); S. Pinsky, B. Sande and J. Hiller, *ibid*, **51**, 726(1995).

[8] T. Sugihara and M. Yahiro, Phys. Rev. **D53**, 7239(1996).

[9] R. J. Perry and K. G. Wilson, Nucl. Phys. **B403**, 587(1993).

[10] R. J. Perry, Ann. Phys. (N.Y.)**232**, 116(1994).

[11] G. P. Lepage, S. J. Brodsky, T. Huang, and P. B. Mackenzie, *Particles and Fields, 2*, edited by A. Z. Capri and A. N. Kamal (Plenum, New York, 1983).

[12] C. Bloch and J. Horowitz, Nucl. Phys. **8**, 91(1958).

[13] K. G. Wilson and J. Kogut, Phys. Rep. **C12**, 75(1974).

[14] D. Callaway and D. Maloot, Phys. Rev. **D27**, 406(1983); L. O'Raifeartaigh, A. Wipf and H. Yoneyama, Nucl. Phys. **B271**, 653(1986); H. Mukaida and Y. Shimada, hep-th/9602086.

[15] H. Bergknoff, Nucl. Phys. **B122**, 215(1977)

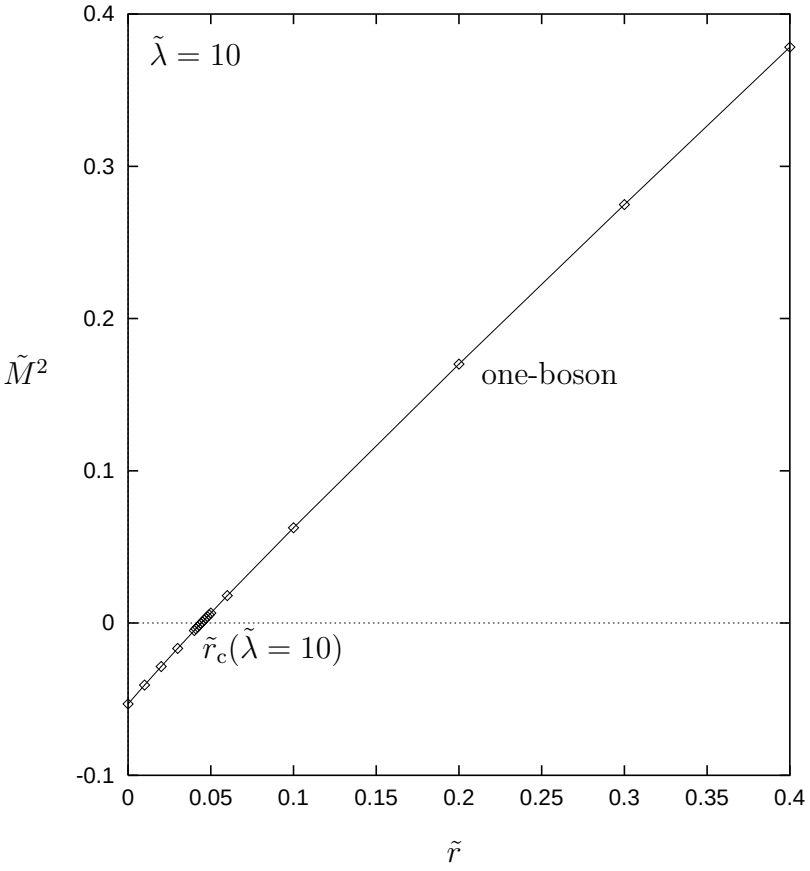


FIG. 1. Mass spectrum for the lowest eigenstate with $\tilde{\lambda} = 10$. The spectrum is plotted as a function of the input mass parameter $\tilde{r}$. $\tilde{r}_c$ is a critical point, which gives the massless ground state.

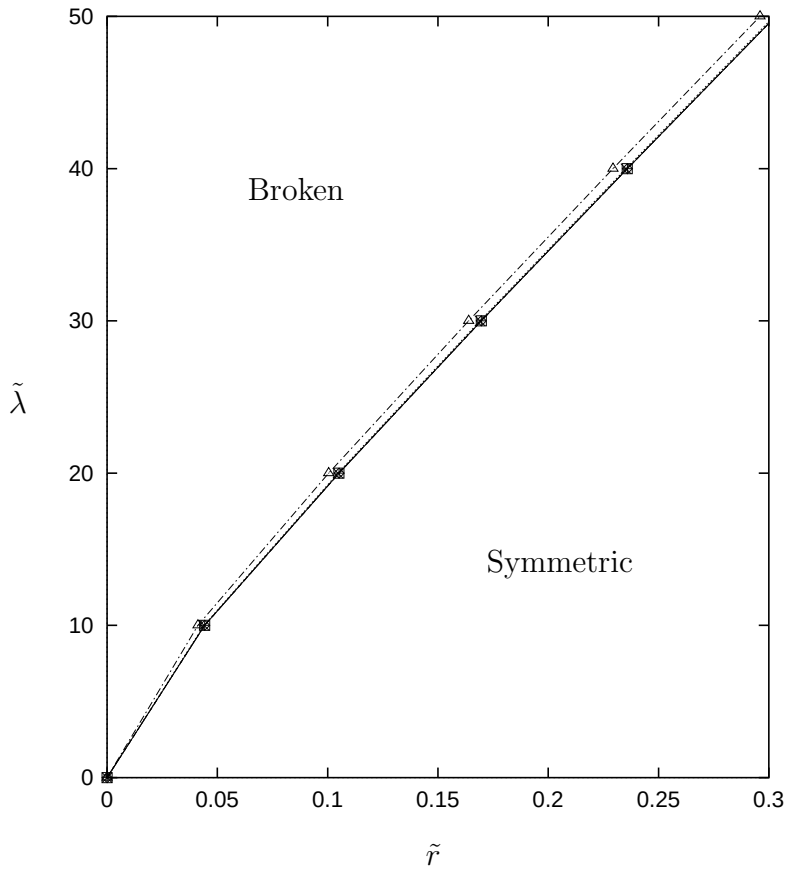


FIG. 2. Critical lines for various values of the marginal coupling constant $\tilde{w}$. The diamonds, bars, squares, crosses and triangles correspond to $\tilde{w} = 0$, $\tilde{w} = 1$, $\tilde{w} = 10$, $\tilde{w} = 10^2$ and $\tilde{w} = 10^3$, respectively. The critical line little depends on the marginal coupling constant.

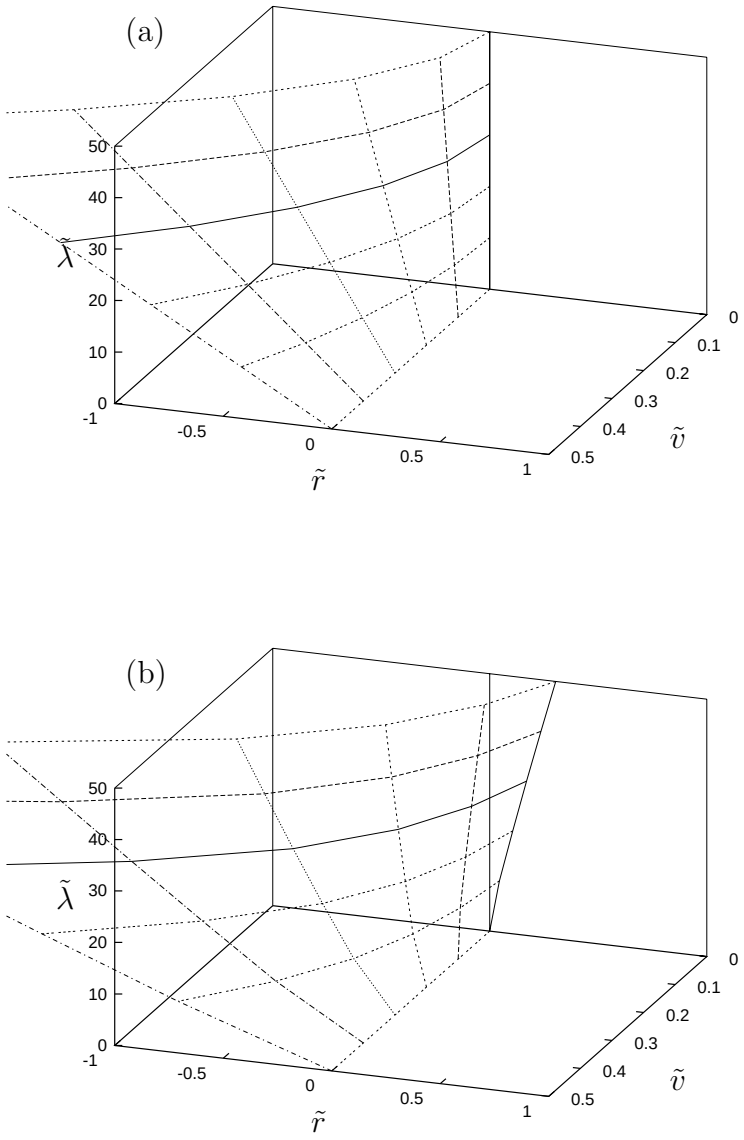


FIG. 3. (a)A surface for the relation $\tilde{\lambda}\tilde{v}^2 + 6\tilde{r} = 0$ is figured. (b)A critical surface, which gives the massless ground state, is calculated by diagonalizing the light-front Hamiltonian in the Fock space truncated up to three-body states.

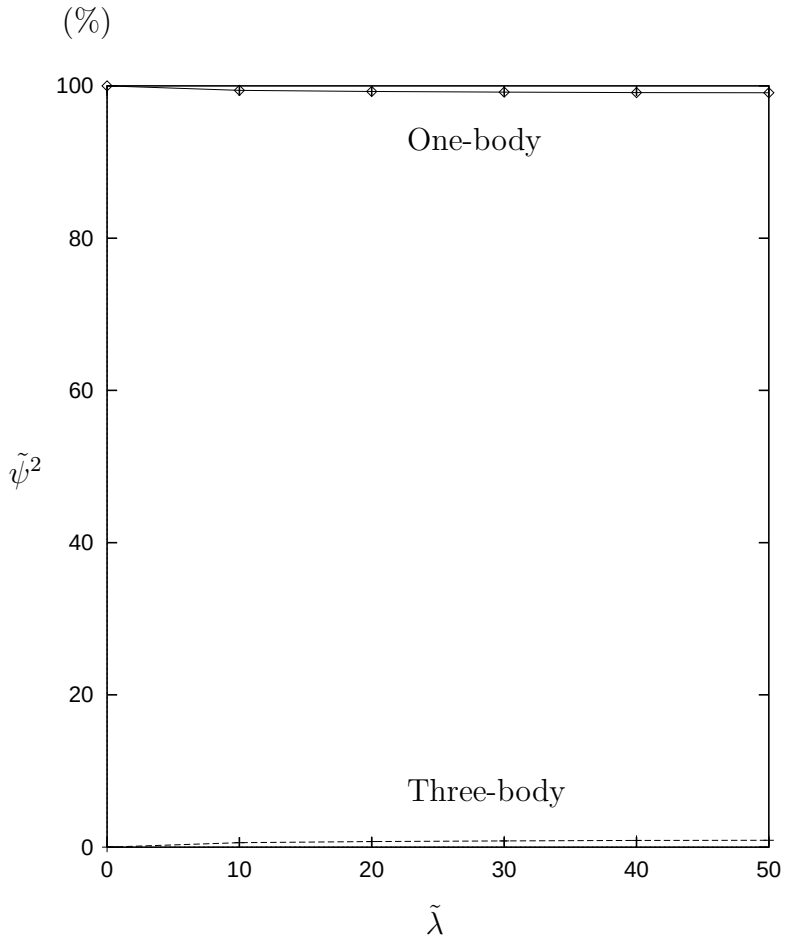


FIG. 4. Wavefunction components of the ground state on the critical line; one- and three-body components are shown by diamonds and crosses as a function of $\tilde{\lambda}$, respectively. Lines are intended to guide the eyes.

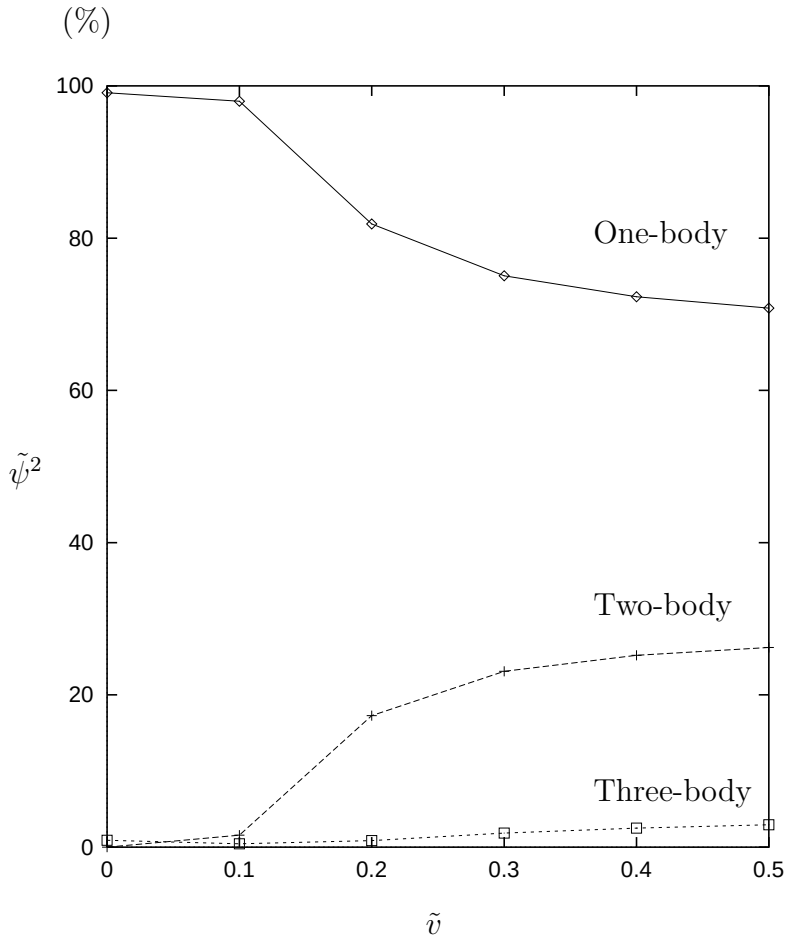


FIG. 5. Wavefunction components of the ground state on the critical line; one-, two- and three-body components on an intersection between the critical surface and the $\tilde{\lambda} = 50$ plane are shown by diamonds, crosses and squares as a function of $\tilde{v}$, respectively. Lines are intended to guide the eyes.

## TABLES

TABLE I. Values of mass parameter $\tilde{r}$ which give massless modes on the $\tilde{v} = 0$ plane are tabulated as a function of $\tilde{\lambda}$ in the cases $\tilde{w} = 0$, $\tilde{w} = 1$, $\tilde{w} = 10$, $\tilde{w} = 10^2$ and $\tilde{w} = 10^3$. The marginal coupling dependence of the critical line is weak.

| $\tilde{w}\backslash\tilde{\lambda}$ | 0.0 | 10.0 | 20.0 | 30.0 | 40.0 | 50.0 |
|---|---|---|---|---|---|---|
| 0.0 | 0.000 | 0.044 | 0.105 | 0.170 | 0.236 | 0.303 |
| $10^0$ | 0.000 | 0.044 | 0.105 | 0.170 | 0.236 | 0.303 |
| $10^1$ | 0.000 | 0.044 | 0.105 | 0.170 | 0.236 | 0.303 |
| $10^2$ | 0.000 | 0.044 | 0.105 | 0.170 | 0.235 | 0.302 |
| $10^3$ | 0.000 | 0.041 | 0.100 | 0.164 | 0.230 | 0.296 |